Improved Visible Light Absorption of Potent Iridium(III) Photooxidants for Excited-State Electron Transfer Chemistry

Robin Bevernaegie,[†] Sara A. M. Wehlin,[‡] Eric J. Piechota,[‡] Michael Abraham,[†] Christian Philouze,[Γ] Gerald J. Meyer,[‡] Benjamin Elias[†]* and Ludovic Troian-Gautier[‡⊥]*

[†]UCLouvain, Institut de la Matière Condensée et des Nanosciences (IMCN), Molecular Chemistry, Materials and Catalysis (MOST), Place Louis Pasteur 1 box L4.01.02, B-1348 Louvain-la-Neuve, Belgium.

[‡]Department of Chemistry, University of North Carolina at Chapel Hill, Chapel Hill, North Carolina, 27599-3290, United States

[Γ]Département de Chimie Moléculaire, Université Grenoble-Alpes (UGA), UMR CNRS 5250, CS 40700, 38058 Grenoble

[⊥]Laboratoire de Chimie Organique, Université Libre de Bruxelles (ULB), CP 160/06, 50 avenue F.D. Roosevelt, B-1050 Brussels, Belgium.

Supporting Information Placeholder

ABSTRACT: Three iridium photosensitizers, $[Ir(dCF_3ppy)_2(N\text{-}N)]^+$, where N-N is 1,4,5,8-tetraazaphenanthrene (TAP), pyrazino[2,3-a]phenazine (pzph) or benzo[a]pyrazino[2,3-h]phenazine (bpph) and dCF_3ppy is 2-(3,5-bis(trifluoromethyl-phenyl)pyridine), were found to be remarkably strong photo-oxidants with enhanced light absorption in the visible region. In particular, judicious ligand design provided access to **Ir-bpph**, with a molar absorption coefficient, $\varepsilon = 9800\ M^{-1}cm^{-1}$, at 450 nm and an excited-state reduction potential, $E(Ir^{+*/0}) = 1.76$ V vs. NHE. These complexes were successful in performing light-driven charge separation and energy storage where each excited-state oxidized seven different electron donors with rate constants between 0.089 to 3.06 $x10^{10}\ M^{-1}s^{-1}$. A Marcus analysis provided a total reorganization energy of 0.7±0.1 eV for excited-state electron transfer.

Since the early 2000s, cyclometalated iridium(III) complexes have emerged as powerful light-emitting materials, with exceptional photostability and highly tunable optoelectronic properties. They have found broad applications in lighting devices,[1-3] life sciences[4-10] and photoredox chemistry,[11-16] however their poor light harvesting in the visible region has largely precluded applications in solar energy conversion. Heteroleptic complexes with the architecture $[Ir(C\text{-}N)_2(N\text{-}N)]^+$ (C-N = cyclometalated ligand, N-N = diimine ligand) have been the focus of intense research because they possess spatially-separated frontier orbitals.[17-18] This is a key advantage that enables the independent tuning of the C-N centered HOMO and N-N centered LUMO levels and hence the related reduction potentials, $E_{1/2}(Ir^{(n/n-1)})$. Potent (photo)oxidants with positive $E_{1/2}(Ir^{(IV/III)})$ or $E_{1/2}(Ir^{+*/0})$ are desired for applications such as water oxidation, hydrohalic acid oxidation, or photoredox catalysis.[19-26] Of particular interest is the energetically demanding aqueous halide oxidation which occurs at $E_{1/2}(X^{\bullet/-})$ of 1.33, 1.93 and > 2V *vs*. NHE for iodide, bromide and chloride, respectively.[25] Unfortunately, due to limited visible light absorption and unsatisfactory thermodynamic properties, existing iridium(III) photosensitizers are of limited use. Efforts to circumvent their poor visible light harvesting include covalently linked additional chromophores[27-29], engineering the HOMO-LUMO gap through ligand modifications[30-33] and changing the nature of the emissive excited states.[34-35] Here, we report access to iridium complexes (**Chart 1** and **Figure 1**) that are strong photo-oxidants with molar absorption coefficient suitable for visible-light-driven applications. Furthermore, excited-state electron transfer studies reported herein reveal a small reorganization energy demonstrating that these new Ir complexes are promising for visible-light-driven applications from both a kinetic and thermodynamic point of view.

The synthetic approach to yield photo-oxidizing iridium complexes with increased visible light absorption relied on several factors. Two trifluoromethyl-substituted phenylpyridine ligands (dCF_3ppy) were chosen to decrease the Ir–C bond electron density and thus increase the photo-oxidizing character. The N-N ligand was systematically extended from the electron-deficient 1,4,5,8-tetraazaphenanthrene (TAP) backbone.[36-37] Conjugation of π-electron density was increased through the addition of one (pyrazino[2,3-a]phenazine, pzph) or two (benzo[a]pyrazino[2,3-h]phenazine, bpph) phenyl rings to TAP. Such annular modifications stabilized the LUMO

level and hence increased visible light absorption independently of the excited-state reduction potential, $E_{1/2}(Ir^{+*/0})$. Moreover, the additional phenyl rings induced intra-ligand charge transfer (ILCT) bands between the phenyl donor groups and the electron-accepting pyrazine cores.[38]

Chart 1. Structures of Ir-TAP, Ir-pzph and Ir-bpph.

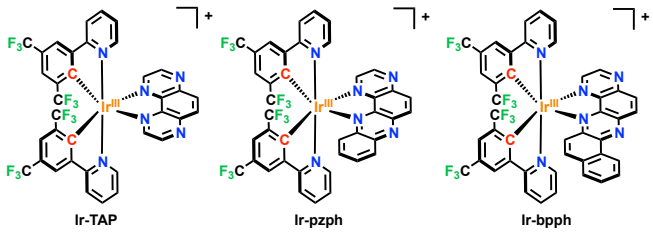

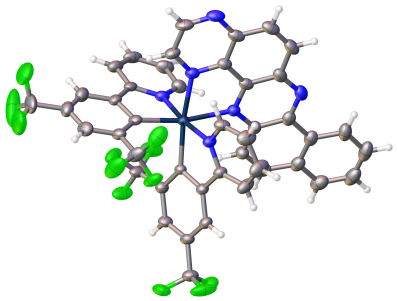

Figure 1. ORTEP diagram for **Ir-bpph** with the ellipsoids drawn at the 50% probability level. A PF_6^- counter ion as well as a diethylether molecule were omitted for clarity.

The synthesis of the three planar ligands was achieved by condensation of 5,6-diamino-quinoxaline with the suitable dione (**Figure S1**). For pzph, this synthetic approach was an improvement compared to the previously published procedure.[39] For the newly-reported bpph, this condensation yielded a mixture of regioisomers in 4:6 proportions, which were separated by chromatography on silica. Subsequently, each complex was formed by successive chelation of the cyclometalated ligands, as described by Nonoyama,[40] followed by addition of the N-N ligand. The three complexes were characterized by strong ligand-centered (LC) absorption bands from 200 to 350 nm while transitions at wavelengths > 350 nm are most often attributed to mixed metal-to-ligand (MLCT) and ligand-to-ligand (LLCT) charge transfer bands from the dCF_3ppy-Ir moiety to the N-N ligand (**Figure 2**).[8, 41] For **Ir-pzph** and **Ir-bpph**, the greater electronic conjugation within the diimine ligand stabilized the Ir(III) LUMO and resulted in both a redshift of the lowest energy absorption feature as well as a significant increase in molar absorption coefficients which reached values of ε_{450} =500 $M^{-1}cm^{-1}$, 1400 $M^{-1}cm^{-1}$ and 9800 $M^{-1}cm^{-1}$ for **Ir-TAP**, **Ir-pzph** and **Ir-bpph** respectively.

Time-dependent density functional theory indicated increased contribution from pzph or bpph intra-ligand charge transfer to these visible absorption bands (**Figures S19-24**). These assignments were strengthened by vibronic structure evident in steady-state photoluminescence spectra (**Figures 2 and S26-27),** as well as their long excited-state lifetimes, τ, and their corresponding small radiative (k_r) and non-radiative (k_{nr}) decay rate constants (**Table 1**).

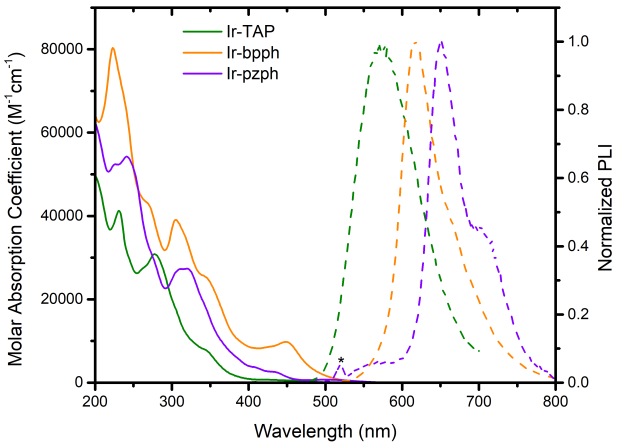

Figure 2. Absorption (solid) and steady-state photoluminescence (dash) spectra of the iridium complexes measured in acetonitrile at room temperature. An excitation wavelength between 400 and 470 nm was used, where the absorbance was below 0.1. * Raman peak of CH_3CN

Reversible electrochemical reduction associated with the N-N ligands were determined by cyclic voltammetry in 0.1 M $TBAPF_6/CH_3CN$ electrolyte and reported *vs.* NHE (**Figure S25**), $E_{1/2}(Ir^{(+/0)})$ = –0.41, –0.13 and –0.25 V for **Ir-TAP**, **Ir-pzph** and **Ir-bpph** respectively (**Table 1**). In all cases, $E_{1/2}(Ir^{(IV/III)})$ was > 2.2 V. An excited-state reduction potential ($E_{1/2}(Ir^{+*/0})$) of *ca.* 1.77 V *vs.* NHE was determined for all three complexes using the $Ir^{(+/0)}$ reduction potentials and a E_{00} value determined through Franck-Condon lineshape analysis of the photoluminescence spectra (**Figures S26-27**).[42-45]

Excited-state reactivity of **Ir-TAP**, **Ir-pzph** and **Ir-bpph** was investigated by time-resolved photoluminescence quenching experiments with seven quenchers. In each case, excited-state quenching was solely dynamic in nature, as indicated by the initial amplitude of the time-resolved photoluminescence.[25-26, 46] A representative example of **Ir-bpph** excited-state quenching with halides is shown in **Figure 3**. Quenching by all other complex/quencher combinations are presented in **Figures S28-S34**. The corresponding quenching rate constants (k_q) obtained through Stern-Volmer analysis ranged from 0.089 to 3.06 $x10^{10}$ $M^{-1}s^{-1}$ (**Table 2**).

Transient absorption spectroscopy was performed with **Ir-TAP**, **Ir-pzph** and **Ir-bpph** and tri-tolylamine (Me-TPA) in argon purged CH_3CN solutions (**Figures S36**). Pulsed light excitation of an Ir complex resulted in electron transfer from Me-TPA as evident through the observation of spectral features unambiguously attributed to the formation of $Me\text{-}TPA^+$, that also provided access to the spectra of the monoreduced iridium species. (**Figures S35-S36**).

Table 1. Photophysical and electrochemical properties of the Ir(III) complexes in acetonitrile.

Complex	ε ($M^{-1}cm^{-1}$)[a]	λ_{em} (nm)	Φ_{em}	k_r (s^{-1})	k_{nr} (s^{-1})	τ (μs)[b]	$Ir^{(+/0)}$ [c]	$Ir^{(+*/0)}$ [c]	E_{00} (eV) [d]
Ir-TAP	*500*	*572*	*0.154*[e]	1.1×10^5	6.0×10^5	*1.4*	*-0.41*	*1.78*	*2.19*
Ir-pzph	*1400*	*651*	*0.028*[f]	2.9×10^3	1.0×10^5	*9.7*	*-0.13*	*1.77*	*1.90*
Ir-bpph	*9800*	*618*	*0.057*[f]	1.2×10^3	2.0×10^4	*47.0*	*-0.25*	*1.76*	*2.01*

[a] at 450 nm. [b] measured at a concentration of 10 μM. [c] V *vs.* NHE. [d] Determined by Franck-Condon lineshape analysis. [e] Measured *vs.* Quinine ($\Phi = 0.546$).[47] [f] Measured *vs.* $[Ru(bpy)_3]^{2+}$.[48]

Table 2. Excited-state quenching rate constants (k_q) for the Ir(III) complexes by various quenchers in CH_3CN.

	$E(D^{n/n-1})$	k_q ($\times 10^{10}$ $M^{-1}s^{-1}$)		
	V vs NHE	*Ir-TAP*	*Ir-pzph*	*Ir-bpph*
H_2Q	*0.70*[a]	*0.84*	*0.67*	*0.65*
MeO-TPA	*0.72*[b]	*1.15*	*1.25*	*1.14*
TPA	*0.93*[b]	*1.17*	*1.34*	*1.21*
I^-	*1.23*[c]	*2.85*	*3.06*	*2.97*
Br^-	*1.35 ± 0.04*[d]	*1.89*	*2.29*	*2.16*
Cl^-	*1.46 ± 0.05*[d]	*0.82*	*1.04*	*0.67*
^{t}Bu-Phenol	*1.50*[e]	*0.26*	*0.16*	*0.089*

[a]from Ref [49]. [b]from Ref [50]. [c]from Ref [51]. [d] this work. [e]from Ref [52].

Additional transient absorption spectroscopy experiments were performed using **Ir-bpph** with iodide, bromide and chloride (**Figure 3**). With iodide and bromide, transient absorption changes were consistent with the formation of monoreduced iridium complex and either $I_2^{\bullet-}$ or $Br_2^{\bullet-}$. UV-Visible spectra before and after transient absorption experiments were superimposable, indicative of the high stability of these iridium complexes. In the case of chloride, excited-state quenching by transient absorption spectroscopy was evident only by a drastic decrease in excited-state lifetime. Unfortunately, photoproducts resulting from electron transfer were not observed even when 100 mJ/pulse of 532 nm light was used.

Quenching rate constants, k_q, were then compiled as a function of the free energy change for the reactions between the quenchers and iridium complexes, $\Delta G^o = \{E_{1/2}(D^{n/n-1}) - E_{1/2}(Ir^{+*/0})\}F$ as shown in **Figure 4A**, when possible as one-electron redox potentials for $Cl^{\bullet/-}$ and $Br^{\bullet/-}$ have not been previously reported in acetonitrile. Though the quenching species were not a homologous series where reaction exergonicities were systematically varied, the driving force for quenching spanned nearly 1 eV and provided impetus to investigate electron transfer reactivity more closely.

Quenching rate constants were found to qualitatively increase with reaction exergonicity before appearing to saturate at intermediate driving forces. Much more interesting was that beyond $-\Delta G^o > 0.8$ eV, k_q was found to decrease, suggestive of Marcus inverted behavior which is rarely observed in bimolecular reactions.[53] For Cl^- and Br^-, the expectation was that they should be more difficult to oxidize than I^-, which has a known one-electron reduction potential of 1.23 eV vs. NHE.[25-26, 51] This expectation was reflected in the Stern-Volmer analysis as smaller k_q for Br^- and Cl^- were observed.

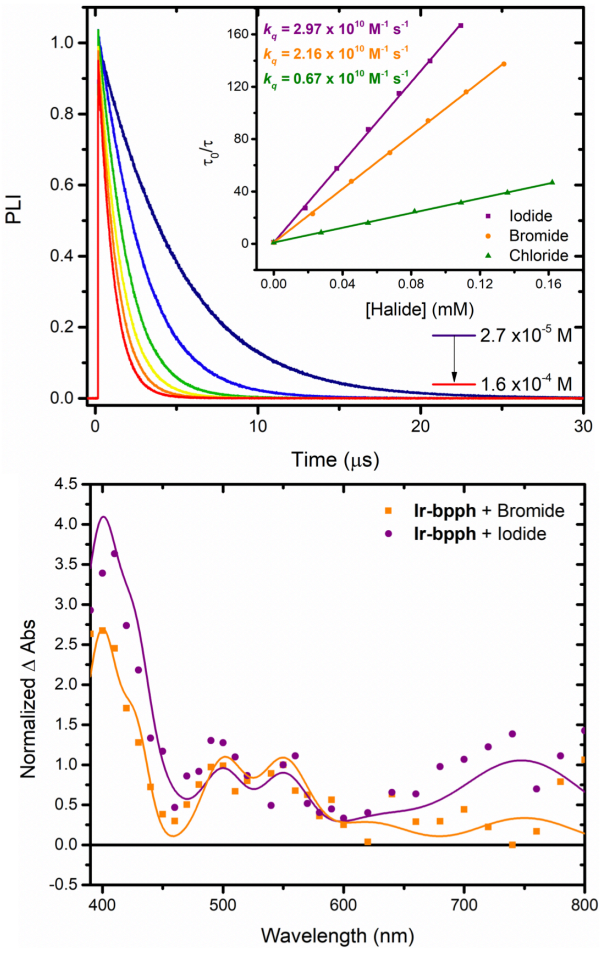

Figure 3. (top) Time-resolved photoluminescence of **Ir-bpph** with increasing amount of TBACl in argon purged acetonitrile at room temperature. The inset represents the Stern-Volmer plots determined for the excited-state quenching of **Ir-bpph** by iodide (purple), bromide (orange) and

chloride (green). (bottom) Transient absorption spectroscopy of **Ir-bpph** in the presence of TBAI (purple) and TBABr (orange). Overlaid are results of spectral modelling based on spectra of $I_2^{\bullet-}$, $Br_2^{\bullet-}$ and monoreduced **Ir-bpph**.

To develop a quantitative investigation into the kinetics of electron transfer, k_q was corrected for diffusional contributions as it is related to the second-order activated rate constant, k_{act}, and the diffusion rate constant, k_{diff}, through **Equation 1**.

$$\frac{1}{k_q} = \frac{1}{k_{act}} + \frac{1}{k_{diff}} \qquad \text{Eq. 1.}$$

Diffusion limits for neutral and charged quenchers were calculated using the Stokes-Einstein equation, and included a Coulombic work term correction.[25, 54-55] In agreement with literature values for diffusion of neutral species in acetonitrile, this was calculated as k_{diff} = 1.9×10^{10} $M^{-1}s^{-1}$,[55] while the value for oppositely charged species, *i.e.* a halide and Ir^+ complex, was estimated to be 5.0×10^{10} $M^{-1}s^{-1}$. Each series appeared to be near a diffusion limit, **Figure 4A**, and application of Eq. 1 allowed to estimate k_{act} for each complex/quencher combination (**Table S7**).

Activated rate constants were determined using k_{diff} for both halide and neutral quenchers and were similarly analyzed as a function of $-\Delta G^o$, **Figure 4B**. Non-adiabatic Marcus theory, **Equation 2**, was used to model k_{act} as a product of one pre-factor, A', total reorganization energy, λ, and free energy change for the reaction, ΔG^o.

$$k_{act} = K_A k_{ET} = A'(\lambda)\exp\left(-\frac{(\Delta G^0+\lambda)^2}{4\lambda k_b T}\right) \qquad \text{Eq. 2.}$$

Two methods were used to examine the experimental data. First, a least-squares analysis of k_{act} with **Equation 2** provided λ = 0.62 eV and A' = 8×10^{10} $M^{-1}s^{-1}$, while excluding the quenching data for Cl^- and Br^-. A second method utilized values of λ = 0.7 eV and a transition state collision frequency of A' = 1×10^{11} $M^{-1}s^{-1}$ commonly utilized for bimolecular electron transfer reactions.[56] From there, k_{act} was calculated over a 1.5 eV driving force range centered on $-\Delta G^o$ = 0.7 eV for both neutral and charged species, shown as the black solid line in **Figure 4B**, under an assumption that A' and λ were independent of the quencher identity. It was evident that a maximum in k_{act} alone revealed that oft-quoted magnitudes of A' = 1×10^{11} $M^{-1}s^{-1}$ for bimolecular reactions was entirely appropriate.[56] Finally, an average k_{act} for Cl^- and Br^- and **Eq. 1** were used to estimate the driving force for the reaction using Cl^- and Br^- which subsequently provided one-electron redox potentials shown in **Table 1**.

In conclusion, the results highlight that through rational ligand design, iridium complexes with $E_{1/2}(Ir^{(IV/III)}) > 2.2$ V, $E(Ir^{+*/0}) = 1.76$ V *vs* NHE and strong visible light harvesting (ε = 9800 $M^{-1}cm^{-1}$ at 450 nm) can be realized and utilized for visible-light-driven chemistry. Nanosecond transient absorption spectroscopy revealed that the photosensitizer excited-states were able to oxidize a variety of organic substrates and halides. Application of Marcus theory provided a small total reorganization energy of 0.7 eV implying small kinetic barriers for excited-state electron transfer. Hence the **Ir-bpph** complex combines enhanced visible light absorption, strong photo-oxidizing power and a small reorganization energy for rapid electron transfer.

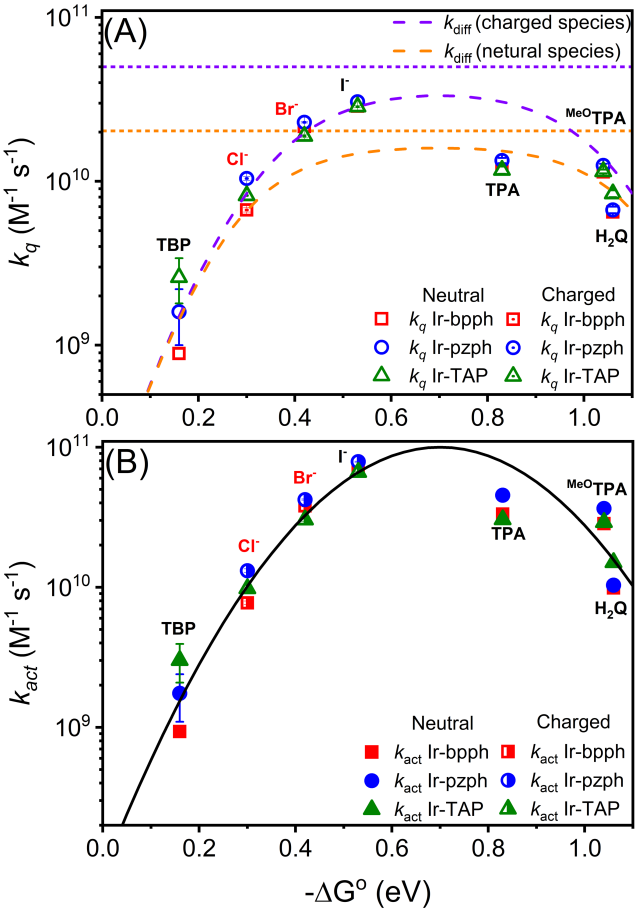

Figure 4. (Top) Experimentally determined k_q values for neutral (empty) and charged (dot-filled shape) species with three Ir^+ complexes as a function of driving force for electron transfer, $-\Delta G^o$. Horizontal dotted lines represent calculated diffusion limits for neutral (orange) and charged (purple) quenchers in CH_3CN solution. The dashed lines represent solutions to **Eq. 1** using the determined values of k_{diff} and simulated values of k_{act}. (Bottom) Activated rate constants calculated by removing the influence of diffusion on experimentally determined k_q. The black solid line is a result from Marcus theory simulations using λ = 0.7 eV and A' = 1×10^{11} $M^{-1}s^{-1}$. k_{act} used to determine $\Delta G°$ and $E_{1/2}(Br^{\bullet/-})$ and $E_{1/2}(Cl^{\bullet/-})$ through **Eq. 1** and **2** are indicated in red.

ASSOCIATED CONTENT

Supporting Information. Experimental section, Electrochemistry, X-Ray crystallography, DFT calculations, Time-resolved photoluminescence quenching, Stern-Volmer plots, Transient absorption spectroscopy. The Supporting Information is available free of charge on the ACS Publications website.

AUTHOR INFORMATION

Corresponding Author

Ludovic.Troian.Gautier@ulb.ac.be, Benjamin.Elias@uclouvain.be

Funding Sources

No competing financial interests have been declared.

ACKNOWLEDGMENT

R. B. and B.E acknowledge the Fonds National pour la Recherche Scientifique (F.R.S.-FNRS), the Fonds pour la Formation à la Recherche dans l'Industrie et dans l'Agriculture (F.R.I.A). L.T.-G. is a Postdoctoral researcher of the Fonds de la Recherche Scientifique – FNRS. Steady-State and time-resolved absorption and photoluminescence experiments were performed using instrumentation in the Alliance for Molecular PhotoElectrode Design for Solar Fuels (AMPED), an Energy Frontier Research Center (EFRC) funded by the U.S. Department of Energy (DOE), Office of Science, Basic Energy Sciences BES, under Award DE-SC0001011. The authors wish to acknowledge the support from the ICMG FR2607, Chemistry Nanobio Platform, Grenoble and in particular Prof. Eric Defrancq.

REFERENCES

1. Li, T.-Y.; Wu, J.; Wu, Z.-G.; Zheng, Y.-X.; Zuo, J.-L.; Pan, Y., Rational design of phosphorescent iridium(III) complexes for emission color tunability and their applications in OLEDs. *Coord. Chem. Rev.* **2018,** *374*, 55-92.

2. Costa, R. D.; Ortí, E.; Bolink, H. J.; Monti, F.; Accorsi, G.; Armaroli, N., Luminescent Ionic Transition-Metal Complexes for Light-Emitting Electrochemical Cells. *Angew. Chem. Int. Ed.* **2012,** *51*, 8178-8211.

3. Henwood, A. F.; Zysman-Colman, E., Lessons learned in tuning the optoelectronic properties of phosphorescent iridium(iii) complexes. *Chem. Commun.* **2017,** *53*, 807-826.

4. Caporale, C.; Massi, M., Cyclometalated iridium(III) complexes for life science. *Coord. Chem. Rev.* **2018,** *363*, 71-91.

5. Deraedt, Q.; Loiseau, F.; Elias, B., Photochemical Tuning of Tris-Bidentate Acridine- and Phenazine-Based Ir(III) Complexes. *J. Fluoresc.* **2016,** *26*, 2095-2103.

6. Zamora, A.; Vigueras, G.; Rodríguez, V.; Santana, M. D.; Ruiz, J., Cyclometalated iridium(III) luminescent complexes in therapy and phototherapy. *Coord. Chem. Rev.* **2018,** *360*, 34-76.

7. Jacques, A.; Kirsch-De Mesmaeker, A.; Elias, B., Selective DNA Purine Base Photooxidation by Bis-terdentate Iridium(III) Polypyridyl and Cyclometalated Complexes. *Inorg. Chem.* **2014,** *53*, 1507-1512.

8. Bevernaegie, R.; Marcélis, L.; Laramée-Milette, B.; De Winter, J.; Robeyns, K.; Gerbaux, P.; Hanan, G. S.; Elias, B., Trifluoromethyl-Substituted Iridium(III) Complexes: From Photophysics to Photooxidation of a Biological Target. *Inorg. Chem.* **2018,** *57*, 1356-1367.

9. Weynand, J.; Bonnet, H.; Loiseau, F.; Ravanat, J.-L.; Dejeu, J.; Defrancq, E.; Elias, B., Targeting G-Rich DNA Structures with Photoreactive Bis-Cyclometallated Iridium(III) Complexes. *Chem-Eur. J.* **2019,** *25*, 12730-12739.

10. Bevernaegie, R.; Doix, B.; Bastien, E.; Diman, A.; Decottignies, A.; Feron, O.; Elias, B., Exploring the Phototoxicity of Hypoxic Active Iridium(III)-Based Sensitizers in 3D Tumor Spheroids. *J. Am. Chem. Soc.* **2019,** *141*, 18486-18491.

11. Shaw, M. H.; Twilton, J.; MacMillan, D. W. C., Photoredox Catalysis in Organic Chemistry. *J. Org. Chem.* **2016,** *81*, 6898-6926.

12. Twilton, J.; Le, C.; Zhang, P.; Shaw, M. H.; Evans, R. W.; MacMillan, D. W. C., The merger of transition metal and photocatalysis. *Nat. Rev. Chem* **2017,** *1*, 0052.

13. Goldsmith, J. I.; Hudson, W. R.; Lowry, M. S.; Anderson, T. H.; Bernhard, S., Discovery and High-Throughput Screening of Heteroleptic Iridium Complexes for Photoinduced Hydrogen Production. *J. Am. Chem. Soc.* **2005,** *127*, 7502-7510.

14. Choi, G. J.; Zhu, Q.; Miller, D. C.; Gu, C. J.; Knowles, R. R., Catalytic alkylation of remote C–H bonds enabled by proton-coupled electron transfer. *Nature* **2016,** *539*, 268.

15. Zheng, J.; Swords, W. B.; Jung, H.; Skubi, K. L.; Kidd, J. B.; Meyer, G. J.; Baik, M.-H.; Yoon, T. P., Enantioselective Intermolecular Excited-State Photoreactions Using a Chiral Ir Triplet Sensitizer: Separating Association from Energy Transfer in Asymmetric Photocatalysis. *J. Am. Chem. Soc.* **2019,** *141*, 13625-13634.

16. Monos, T. M.; Stephenson, C. R. J., Photoredox Catalysis of Iridium(III)-Based Photosensitizers. In *Iridium(III) in Optoelectronic and Photonics Applications*, Zysman-Colman, E., Ed. John Wiley & Sons Ltc.: Chichester, West Sussex, **2017**; pp 541-581.

17. Flamigni, L.; Barbieri, A.; Sabatini, C.; Ventura, B.; Barigelletti, F., Photochemistry and Photophysics of Coordination Compounds: Iridium. In *Photochemistry and Photophysics of Coordination Compounds II*, Balzani, V.; Campagna, S., Eds. Springer Berlin Heidelberg: Berlin, Heidelberg, **2007**; pp 143-203.

18. Deaton, J. C.; Castellano, F. N., Archetypal Iridium(III) Compounds for Optoelectronic and Photonic Applications. In *Iridium(III) in Optoelectronic and Photonics Applications*, Zysman-Colman, E., Ed. John Wiley & Sons Ltc.: Chichester, West Sussex, **2017**; pp 1-69.

19. Kagalwala, H. N.; Chirdon, D. N.; Bernhard, S., Solar Fuel Generation. In *Iridium(III) in Optoelectronic and Photonics Applications*, Zysman-Colman, E., Ed. John Wiley & Sons Ltd.: Chichester, West Sussex, **2017**; pp 583-615.

20. Curtin, P. N.; Tinker, L. L.; Burgess, C. M.; Cline, E. D.; Bernhard, S., Structure−Activity Correlations Among Iridium(III) Photosensitizers in a Robust Water-Reducing System. *Inorg. Chem.* **2009,** *48*, 10498-10506.

21. Metz, S.; Bernhard, S., Robust photocatalytic water reduction with cyclometalated Ir(iii) 4-vinyl-2,2′-bipyridine complexes. *Chem. Commun.* **2010,** *46*, 7551-7553.

22. Baranoff, E.; Yum, J.-H.; Jung, I.; Vulcano, R.; Grätzel, M.; Nazeeruddin, M. K., Cyclometallated Iridium Complexes as Sensitizers for Dye-Sensitized Solar Cells. *Chem-Asian J.* **2010,** *5*, 496-499.

23. Dragonetti, C.; Valore, A.; Colombo, A.; Righetto, S.; Trifiletti, V., Simple novel cyclometallated iridium complexes for potential application in dye-sensitized solar cells. *Inorg. Chim. Acta* **2012,** *388*, 163-167.

24. Ning, Z.; Zhang, Q.; Wu, W.; Tian, H., Novel iridium complex with carboxyl pyridyl ligand for dye-sensitized solar cells: High fluorescence intensity, high electron injection efficiency? *J. Organomet. Chem.* **2009,** *694*, 2705-2711.

25. Troian-Gautier, L.; Turlington, M. D.; Wehlin, S. A. M.; Maurer, A. B.; Brady, M. D.; Swords, W. B.; Meyer, G. J., Halide Photoredox Chemistry. *Chem. Rev.* **2019,** *119*, 4628-4683.

26. Troian-Gautier, L.; Swords, W. B.; Meyer, G. J., Iodide Photoredox and Bond Formation Chemistry. *Acc. Chem. Res.* **2019,** *52*, 170-179.

27. Costa, R. D.; Céspedes-Guirao, F. J.; Bolink, H. J.; Fernández-Lázaro, F.; Sastre-Santos, Á.; Ortí, E.; Gierschner, J., A Deep-Red-Emitting Perylenediimide−Iridium-Complex Dyad: Following the Photophysical Deactivation Pathways. *J. Phys. Chem. C* **2009,** *113*, 19292-19297.

28. Yarnell, J. E.; McCusker, C. E.; Leeds, A. J.; Breaux, J. M.; Castellano, F. N., Exposing the Excited-State Equilibrium in an IrIII Bichromophore: A Combined Time Resolved Spectroscopy and Computational Study. *Eur. J. Inorg. Chem.* **2016,** *2016*, 1808-1818.

29. Takizawa, S.-y.; Ikuta, N.; Zeng, F.; Komaru, S.; Sebata, S.; Murata, S., Impact of Substituents on Excited-State and

Photosensitizing Properties in Cationic Iridium(III) Complexes with Ligands of Coumarin 6. *Inorg. Chem.* **2016,** *55*, 8723-8735.

30. Hasan, K.; Zysman-Colman, E., Panchromic Cationic Iridium(III) Complexes. *Inorg. Chem.* **2012,** *51*, 12560-12564.

31. Lentz, C.; Schott, O.; Auvray, T.; Hanan, G.; Elias, B., Photocatalytic Hydrogen Production Using a Red-Absorbing Ir(III)–Co(III) Dyad. *Inorg. Chem.* **2017,** *56*, 10875-10881.

32. Wang, Y.; Zhao, X.; Zhao, Y.; Yang, T.; Liu, X.; Xie, J.; Li, G.; Zhu, D.; Tan, H.; Su, Z., Photosensitizers based on Ir(III) complexes for highly efficient photocatalytic hydrogen generation. *Dyes Pigments* **2019,** *170*, 107547.

33. Lentz, C.; Schott, O.; Auvray, T.; Hanan, G. S.; Elias, B., Design and photophysical studies of iridium(iii)–cobalt(iii) dyads and their application for dihydrogen photo-evolution. *Dalton Trans.* **2019,** *48*, 15567-15576.

34. Fan, S.; Zong, X.; Shaw, P. E.; Wang, X.; Geng, Y.; Smith, A. R. G.; Burn, P. L.; Wang, L.; Lo, S.-C., Energetic requirements of iridium(iii) complex based photosensitisers in photocatalytic hydrogen generation. *Phys. Chem. Chem. Phys.* **2014,** *16*, 21577-21585.

35. Yuan, Y.-J.; Zhang, J.-Y.; Yu, Z.-T.; Feng, J.-Y.; Luo, W.-J.; Ye, J.-H.; Zou, Z.-G., Impact of Ligand Modification on Hydrogen Photogeneration and Light-Harvesting Applications Using Cyclometalated Iridium Complexes. *Inorg. Chem.* **2012,** *51*, 4123-4133.

36. Kajouj, S.; Marcelis, L.; Lemaur, V.; Beljonne, D.; Moucheron, C., Photochemistry of ruthenium(ii) complexes based on 1,4,5,8-tetraazaphenanthrene and 2,2[prime or minute]-bipyrazine: a comprehensive experimental and theoretical study. *Dalton Trans.* **2017,** *46*, 6623-6633.

37. Troian-Gautier, L.; Moucheron, C., RutheniumII Complexes bearing Fused Polycyclic Ligands: From Fundamental Aspects to Potential Applications. *Molecules* **2014,** *19*, 5028-5087.

38. Foxon, S. P.; Alamiry, M. A. H.; Walker, M. G.; Meijer, A. J. H. M.; Sazanovich, I. V.; Weinstein, J. A.; Thomas, J. A., Photophysical Properties and Singlet Oxygen Production by Ruthenium(II) Complexes of Benzo[i]dipyrido[3,2-a:2′,3′-c]phenazine: Spectroscopic and TD-DFT Study. *J. Phys. Chem. A* **2009,** *113*, 12754-12762.

39. Pietra, S.; Casiraghi, G., Reazioni Nucleofile Sulla 2-nitrofenazina - Nota III. *Gazz. Chim. Ital.* **1967,** *97*, 1826-1836.

40. Matsuo, N., Benzo[h]quinolin-10-yl-N Iridium(III) Complexes. *B. Chem. Soc. Jpn.* **1974,** *47*, 767-768.

41. Bevernaegie, R.; Marcélis, L.; Moreno-Betancourt, A.; Laramée-Milette, B.; Hanan, G. S.; Loiseau, F.; Sliwa, M.; Elias, B., Ultrafast charge transfer excited state dynamics in trifluoromethyl-substituted iridium(iii) complexes. *Phys. Chem. Chem. Phys.* **2018,** *20*, 27256-27260.

42. Troian-Gautier, L.; Marcelis, L.; De Winter, J.; Gerbaux, P.; Moucheron, C., Two ruthenium complexes capable of storing multiple electrons on a single ligand - photophysical, photochemical and electrochemical properties of [Ru(phen)2(TAPHAT)]2+ and [Ru(phen)2(TAPHAT)Ru(phen)2]4+. *Dalton Trans.* **2017,** *46*, 15287-15300.

43. Motley, T. C.; Troian-Gautier, L.; Brennaman, M. K.; Meyer, G. J., Excited-State Decay Pathways of Tris(bidentate) Cyclometalated Ruthenium(II) Compounds. *Inorg. Chem.* **2017,** *56*, 13579-13592.

44. Ito, A.; Meyer, T. J., The Golden Rule. Application for fun and profit in electron transfer, energy transfer, and excited-state decay. *Phys. Chem. Chem. Phys.* **2012,** *14*, 13731-13745.

45. Kober, E. M.; Caspar, J. V.; Lumpkin, R. S.; Meyer, T. J., Application of the energy gap law to excited-state decay of osmium(II)-polypyridine complexes: calculation of relative nonradiative decay rates from emission spectral profiles. *J. Phys. Chem* **1986,** *90*, 3722-3734.

46. Lakowicz, J. R., *Principles of Fluorescence Spectroscopy*. Springer US, New York: 2006.

47. Brouwer Albert, M., Standards for photoluminescence quantum yield measurements in solution (IUPAC Technical Report). In *Pure and Applied Chemistry*, 2011; Vol. 83, p 2213.

48. Ishida, H.; Tobita, S.; Hasegawa, Y.; Katoh, R.; Nozaki, K., Recent advances in instrumentation for absolute emission quantum yield measurements. *Coord. Chem. Rev.* **2010,** *254*, 2449-2458.

49. Eggins, B. R., Interpretation of electrochemical reduction and oxidation waves of quinone–hydroquinone system in acetonitrile. *J. Chem. Soc. Chem. Comm.* **1969**, 1267-1268.

50. DiMarco, B. N.; Troian-Gautier, L.; Sampaio, R. N.; Meyer, G. J., Dye-sensitized electron transfer from TiO2 to oxidized triphenylamines that follows first-order kinetics. *Chem. Sci.* **2018,** *9*, 940-949.

51. Rowley, J. G.; Farnum, B. H.; Ardo, S.; Meyer, G. J., Iodide Chemistry in Dye-Sensitized Solar Cells: Making and Breaking I−I Bonds for Solar Energy Conversion. *J. Phys. Chem. Lett.* **2010,** *1*, 3132-3140.

52. Osako, T.; Ohkubo, K.; Taki, M.; Tachi, Y.; Fukuzumi, S.; Itoh, S., Oxidation Mechanism of Phenols by Dicopper−Dioxygen (Cu2/O2) Complexes. *J. Am. Chem. Soc.* **2003,** *125*, 11027-11033.

53. Piechota, E. J.; Meyer, G. J., Introduction to Electron Transfer: Theoretical Foundations and Pedagogical Examples. *J. Chem. Ed.* **2019,** *96*, 2450-2466.

54. Wehlin, S. A. M.; Troian-Gautier, L.; Li, G.; Meyer, G. J., Chloride Oxidation by Ruthenium Excited-States in Solution. *J. Am. Chem. Soc.* **2017,** *139*, 12903-12906.

55. Murov, S. L.; Carmichael, I.; Hug, G. L., *Handbook of Photochemistry, 2nd edition*. Marcel Dekker, Inc.,New York: 1993.

56. Sutin, N., Nuclear, electronic, and frequency factors in electron transfer reactions. *Acc. Chem. Res.* **1982,** *15*, 275-282.
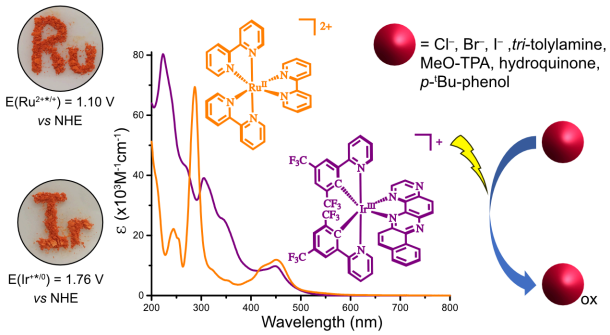
For Table of Content Use Only